Supporting Information

exTTF-Based Dyes Absorbing over the Whole Visible Spectrum

Pierre-Antoine Bouit, Carmen Villegas, Juan Luis Delgado, Pedro M. Viruela, Rosendo Pou-Amérigo, Enrique Ortí,* Nazario Martín*

Dr. P.-A. Bouit, C. Villegas, Dr. J. L. Delgado,[+] Prof. Dr. N. Martín[+]
Departamento de Química Orgánica, Facultad de Química, Universidad Complutense de Madrid, 28040 Madrid (Spain)
Fax: (+34)913944103
E-mail: nazmar@quim.ucm.es
+IMDEA-nanociencia, Facultad de Ciencias, Módulo C-IX, 3ª planta, Ciudad Universitaria de Cantoblanco, 28049 Madrid (Spain)
Homepage: http://www.ucm.es/info/fullerene

Dr. P. M. Viruela, Dr. R. Pou-Amérigo, Prof. Dr. E. Ortí
Instituto de Ciencia Molecular, Universidad de Valencia, 46980 Paterna (Spain)
Fax: (+34)963543274
E-mail: enrique.orti@uv.es

1. Experimental Section

General. Microwave reactions were performed on an Anton Paar "Monowave 300". NMR spectra were recorded at room temperature on a Bruker DPX 300 MHz (^{1}H: 300 MHz; ^{13}C: 75 MHz). Data are listed in parts per million (ppm) and are reported relative to tetramethylsilane (^{1}H, ^{13}C), residual solvent peaks being used as internal standard (CHCl$_3$ ^{1}H: 7.26 ppm, ^{13}C: 77.36 ppm, CDCl$_3$). High resolution mass spectrometry measurements were performed at the Unidad de Espectrometría de Masas of Universidad Complutense de Madrid. Column Chromatography was performed on Merck 60 (40-63 μm) silica. UV-vis spectra were recorded in a Varian Cary 50 spectrometer at a constant temperature of 25 °C in diluted dichloromethane solution (*ca.* 10^{-6} mol L^{-1}). Compounds **1a-b**[1] and **2**[2] were prepared according to published procedures.
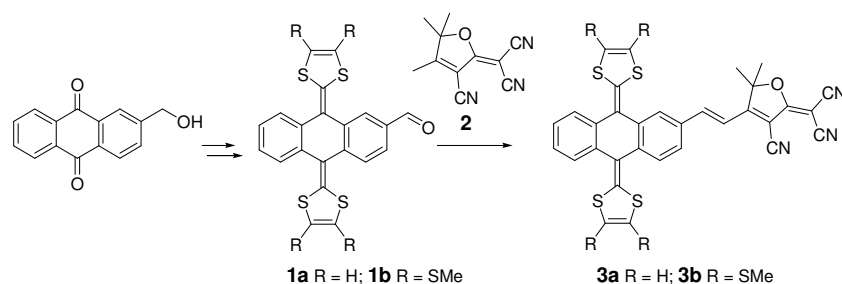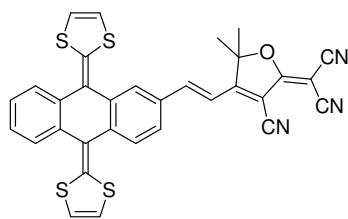

Figure S1. Synthesis of **3a-b**

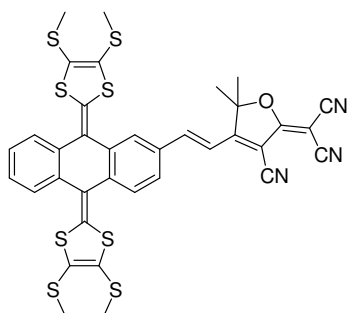Synthesis of **3a** (general procedure for the microwave-assisted Knoevenagel condensation):

1a (30 mg, 0.073 mmol, 1 eq.) and **2** (22 mg, 1.5 eq.) were dissolved in 2 mL of chloroform. 200 mg of silica were added. The reaction was irradiated in the microwave at 110º for 2h. The solvents were evaporated and the crude was purified by chromatography on silica gel using dichloromethane as eluent to afford **3a** as a dark green solid (20 mg, 46 %).

[1] Martín, N.; Pérez, I.; Sánchez, L.; Seoane, C. J. *J Org. Chem*. **1997**, *62*, 5690–5695.
[2] Melikian, G; Rouessac, F.P., Alexandre, C. *Synth. Commun*. **1995**, 25, 3045–3051.

^{1}H NMR (300 MHz, CDCl$_3$): δ 1.80 (s, 6H); 6.31 (d, J = 7 Hz, 1H); 6.36 (d, J = 7 Hz, 1H); 6.39 (s, 2H); 7.05 (d, J = 16 Hz, 1H); 7.30–7.35 (m, 2H); 7.53 (dd, J= 8 Hz, J = 2Hz, 1H); 7.67 (d, J = 16 Hz, 1H); 7.70–7.75 (m, 2H); 7.82 (d, J = 8 Hz, 1H); 7.95 (d, J = 2 Hz, 1H); ^{13}C NMR (75 MHz, CDCl$_3$): δ 28.6; 57.6; 97.6; 99.4; 110.4; 111.0; 111.8; 114.4; 116.8; 117.6; 117.8; 117.9; 120.7; 121.3; 124.9; 125.0; 125.2; 125.9; 126.4; 126.5; 127.3; 131.2; 134.9; 135.0; 136.7; 137.8; 140.1; 140.2; 146.9; 173.6; 175.4. MS (ESI+): [M]$^+$ = 589.04097 (calcd. for C$_{32}$H$_{19}$N$_3$OS$_4$: 589.04055). IR (KBr pellet) ν$_{(C≡N)}$ = 2226 cm^{-1}.

3b was synthesized using the general procedure for the microwave-assisted Knoevenagel condensation (yield = 41 %).

^{1}H NMR (300 MHz, CDCl$_3$): δ 1.82 (s, 3H); 1.84 (s, 3H); 2.41 (s, 12H); 7.08 (d, J = 16 Hz, 1H); 7.34–7.37 (m, 2H); 7.54–7.68 (m, 5H); 7.80 (d, J =1 Hz, 1H); ^{13}C NMR (75 MHz, CDCl$_3$): δ 19.5; 19.6; 19.7; 27.0; 58.3; 98.0; 100.4; 110.6; 111.3; 112.1; 115.3; 122.5; 122.5; 123.0; 125.2; 125.7; 125.8; 125.9; 126.5; 126.7; 127.1; 127.2; 127.8; 127.9; 132.0; 133.7; 134.5; 134.6; 135.8; 136.3; 139.5; 146.8; 173.8; 175.6. MS (ESI+): [M]$^+$ = 772.99368 (calcd. for C$_{36}$H$_{27}$N$_3$OS$_8$: 772.99198). IR (KBr pellet) ν$_{(C≡N)}$ = 2224 cm^{-1}.
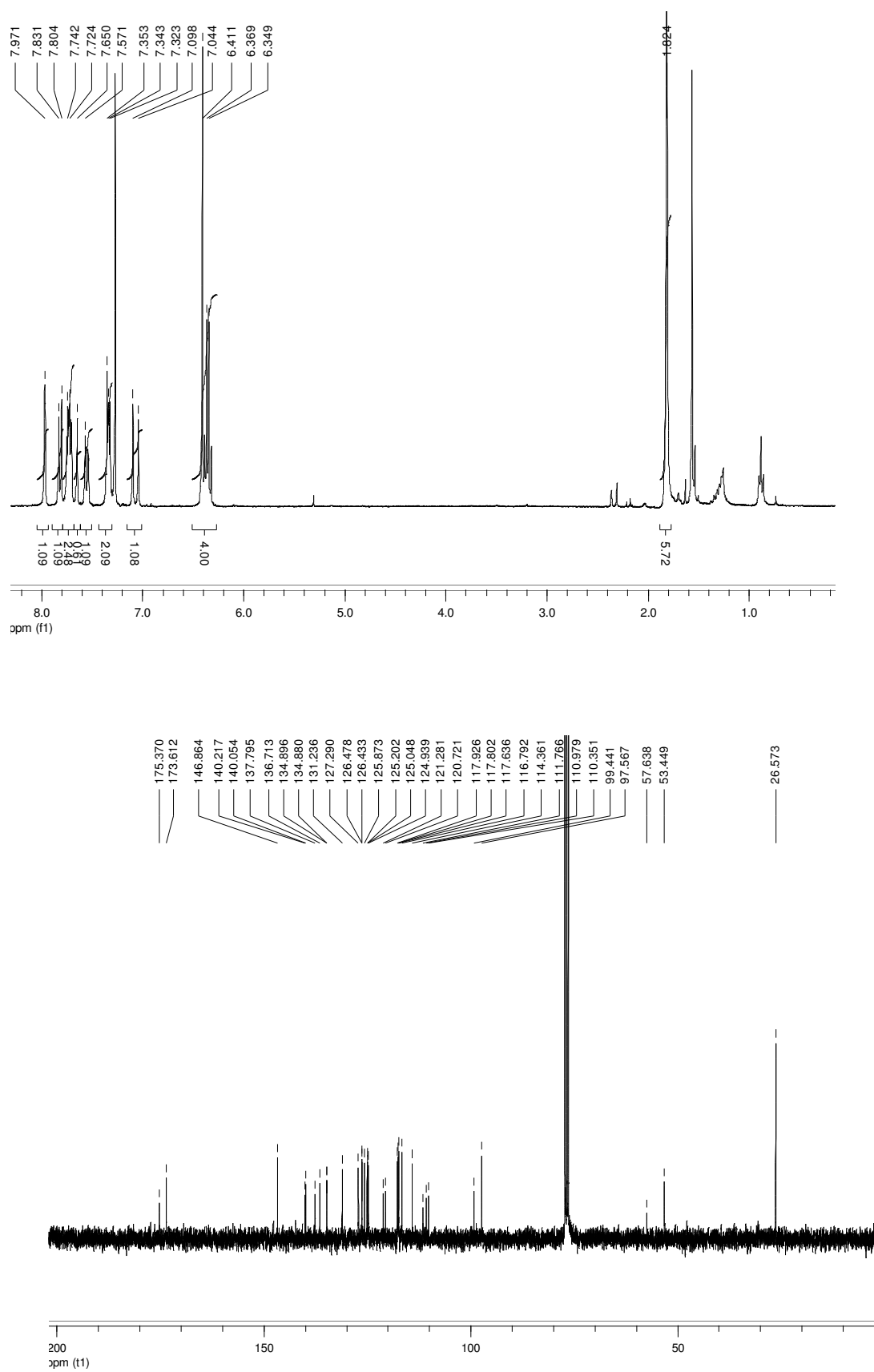
Figure S2. ^{1}H NMR (300 MHz, CDCl$_3$), ^{13}C NMR (75 MHz, CDCl$_3$) of **3a**
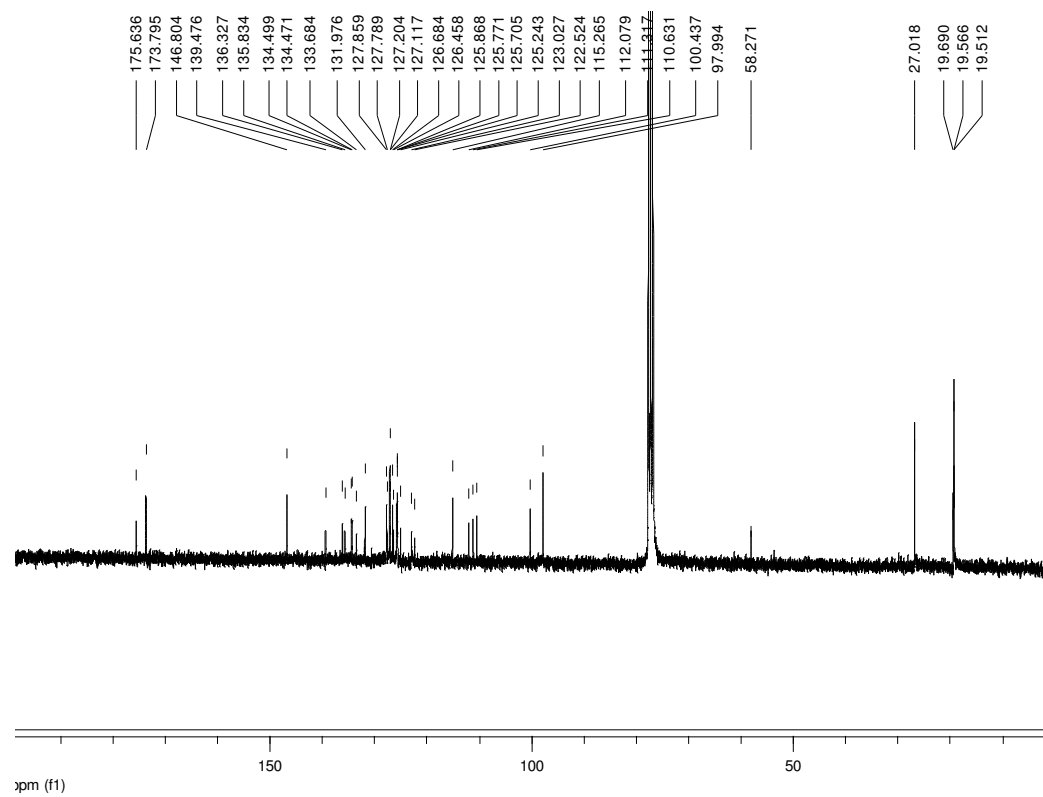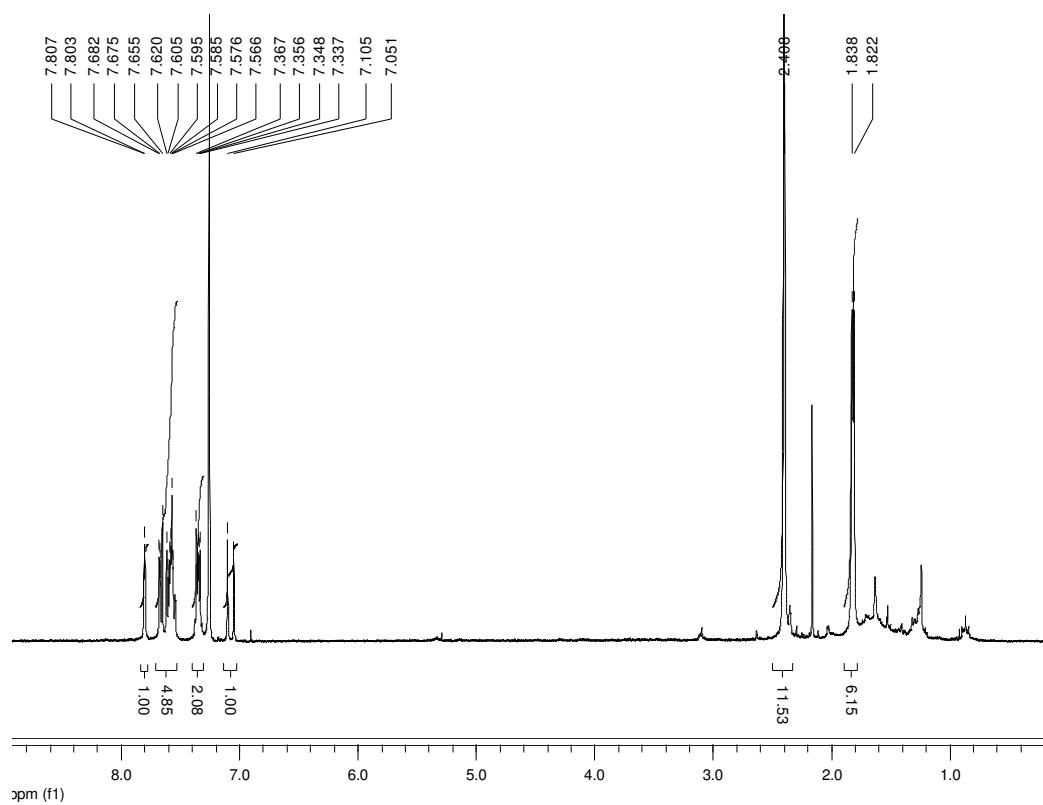
Figure S3. ^{1}H NMR (300 MHz, CDCl$_3$), ^{13}C NMR (75 MHz, CDCl$_3$) of **3b**

Electrochemistry. Cyclic voltammograms were recorded on a potentiostat/galvanostat AUTOLAB with PGSTAT30 equipped with a software GPES for windows version 4.8 in a conventional three compartment cell. Measurements were carried out using a GCE (glassy carbón electrode) as working electrode, a Ag/AgNO$_3$ reference electrode, and a platinum wire as counter electrode. Bu$_4$NClO$_4$ was used as supporting electrolyte and acetonitrile as solvent.
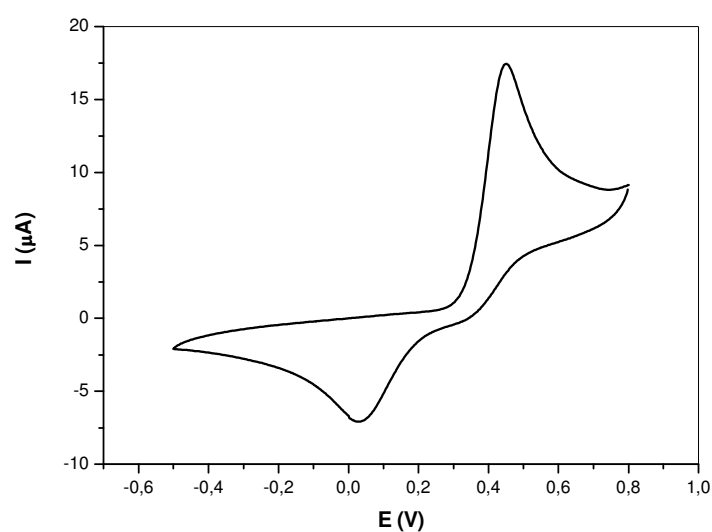

Figure S4. CV trace obtained for the reference exTTF compound (CH$_3$CN, 0.1 M Bu$_4$NClO$_4$, v = 100 mV s^{-1}, V vs. Ag/AgNO$_3$).
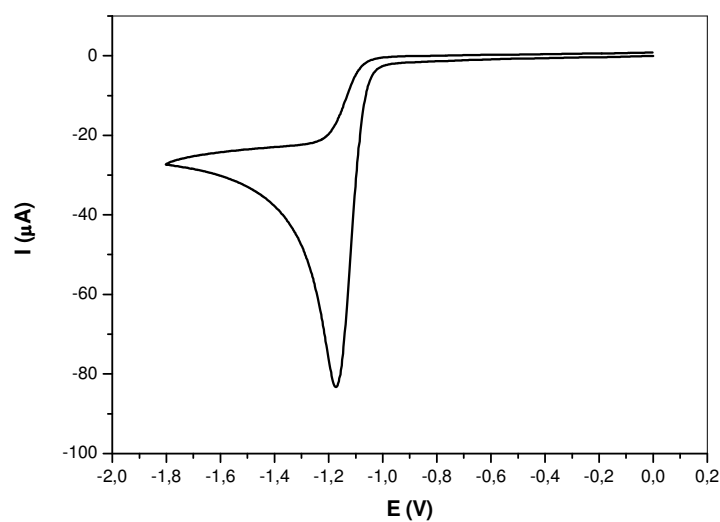
Figure S5. CV trace obtained for compound **2** (CH$_3$CN, 0.1 M Bu$_4$NClO$_4$, v = 100 m V s^{-1}, V vs. Ag/AgNO$_3$).
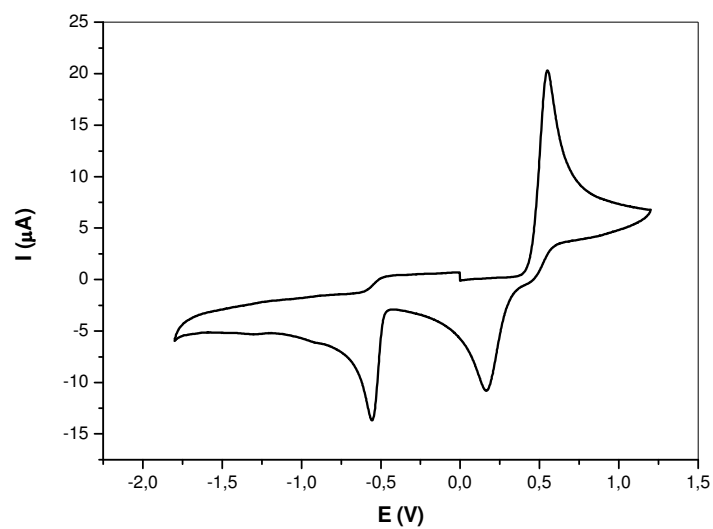
Figure S6. CV trace obtained for **3b** (CH_3CN, 0.1 M Bu_4NClO_4, v = 100 m V s^{-1}, V vs. $Ag/AgNO_3$).

Table S1. Electrochemical data

compound	E_{ox} (V)	E_{red} (V)
exTTF	0.24	-
2	-	−1.17
3a	0.25	−0.56
3b	0.35	−0.55

2. Theoretical Section

All theoretical calculations were carried out within the density functional theory (DFT) approach by using the A.02 revision of the Gaussian 09 program package.[3] Geometry optimizations were performed with Becke's three-parameter B3LYP exchange-functional[4] and the 6-31G** basis set.[5] Net atomic charges were calculated using the natural population analysis (NPA) included in the natural bond orbital (NBO) algorithm proposed by Weinhold and co-workers.[6] Molecular orbitals were plotted using Molekel 4.3.[7]

The molecular geometries of compounds **3a** and **3b** were optimized together of those of the reference compounds exTTF (C_{2v} symmetry) and **2** (C_s symmetry) for comparison purposes. The exTTF unit in compound **3a** adopts a butterfly- or saddle-like structure, similar to that calculated for unsubstituted exTTF. To relieve the short contacts between the sulfur atoms and the hydrogen atoms in the *peri* positions, the central ring of the anthracene unit folds in a boat conformation along the C9–C10 vector by an average angle of 38.4° very similar to that obtained for exTTF (38.8°). The dithiole rings are tilted by 34.2° with respect to the plane defined by the anthracene atoms C11–C12–C13–C14. Furthermore, the dithiole rings are folded inward by 6.7° and 8.6° along the S–S axes. Almost identical folding angles are obtained for **3b**, but this molecule presents a larger bending of the dithiole rings along the S–S axes (18.7°) due to the presence of the SMe substituents. Both for **3a** and **3b**, it is found that the TCF moiety,

[3] Gaussian 09, Revision A.02, Frisch, M. J.; Trucks, G. W.; Schlegel, H. B.; Scuseria, G. E.; Robb, M. A.; Cheeseman, J. R.; Scalmani, G.; Barone, V.; Mennucci, B.; Petersson, G. A.; Nakatsuji, H.; Caricato, M.; Li, X.; Hratchian, H. P.; Izmaylov, A. F.; Bloino, J.; Zheng, G.; Sonnenberg, J. L.; Hada, M.; Ehara, M.; Toyota, K.; Fukuda, R.; Hasegawa, J.; Ishida, M.; Nakajima, T.; Honda, Y.; Kitao, O.; Nakai, H.; Vreven, T.; Montgomery, Jr., J. A.; Peralta, J. E.; Ogliaro, F.; Bearpark,V; Heyd, J. J.; Brothers, E.; Kudin, K. N.; Staroverov, V. N.; Kobayashi, R.; Normand, J.; Raghavachari, K.; Rendell, A.; Burant, J. C.; Iyengar, S. S.; Tomasi, J.; Cossi, M.; Rega, N.; Millam, J. M.; Klene, M.; Knox, J. E.; Cross, J. B.; Bakken, V.; Adamo, C.; Jaramillo, J.; Gomperts, R.; Stratmann, R. E.; Yazyev, O.; Austin, A. J.; Cammi, R.; Pomelli, C.; Ochterski, J. W.; Martin, R. L.; Morokuma, K.; Zakrzewski, V. G.; Voth, G. A.; Salvador, P.; Dannenberg, J. J.; Dapprich, S.; Daniels, A. D.; Farkas, O.; Foresman, J. B.; Ortiz, J. V.; Cioslowski, J.; Fox, D. J., Gaussian, Inc., Wallingford CT, 2009.

[4] a) Becke, A. D. *J. Chem. Phys.* **1993**, *98*, 5648–5652. b) Lee, C.; Yang, W.; Parr, R. G. *Phys. Rev. B* **1988**, *37*, 785–789.

[5] Francl, M. M.; Pietro, W. J.; Hehre, W. J.; Binkley, J. S.; Gordon, M. S.; Defrees, D. J.; Pople, J. A. *J. Chem. Phys.* **1982**, *77*, 3654–3665.

[6] a) Reed, A. E.; Weinhold, F. *J. Chem. Phys.* **1983**, *78*, 4066–4073. b) Reed, A. E.; Weinstock, R. B.; Weinhold, F. *J. Chem. Phys.* **1985**, *83*, 735–746. c) Reed, A. E.; Curtiss, L. A.; Weinhold, F. *Chem. Rev.* **1988**, *88*, 899–926.

[7] Flukiger, P.; Lüthi, H. P.; Portmann, S.; Weber, J., MOLEKEL 4.3; Swiss Center for Scientific Computing, Manno, Switzerland, **2002**.

the ethylene bridge, and one of the benzene rings of the anthracene unit are coplanar with maximum deviations of 1.1° from planarity.

Figure S7a shows the optimized values obtained for selected bond lengths of compound **3a**. The lateral benzene rings of the anthracene unit of the exTTF moiety present an aromatic structure since all the C–C bonds have a length of 1.40±0.02 Å. The ethylene bridge has a special effect on the geometry of the electron-acceptor moiety since it defines a conjugated oligoenic chain with the TCF unit. As shown in Figure S7, the C=C double bonds of the TCF unit lengthen in passing from **2** to **3a** and the C–C single bonds shorten. The increase in the extension of π-conjugation determines that the LUMO of **3a** (–3.22 eV) is calculated at lower energies than the LUMO of **2** (–2.86 eV). This explains the fact that compounds **3a** and **3b** undergo reduction at significantly less negative potentials (–0.56 and –0.55 V, respectively) compared to **2** (–1.17 V) despite the charge transfer of 0.20e that takes place from the exTTF unit to the TCF moiety in the electronic ground state.
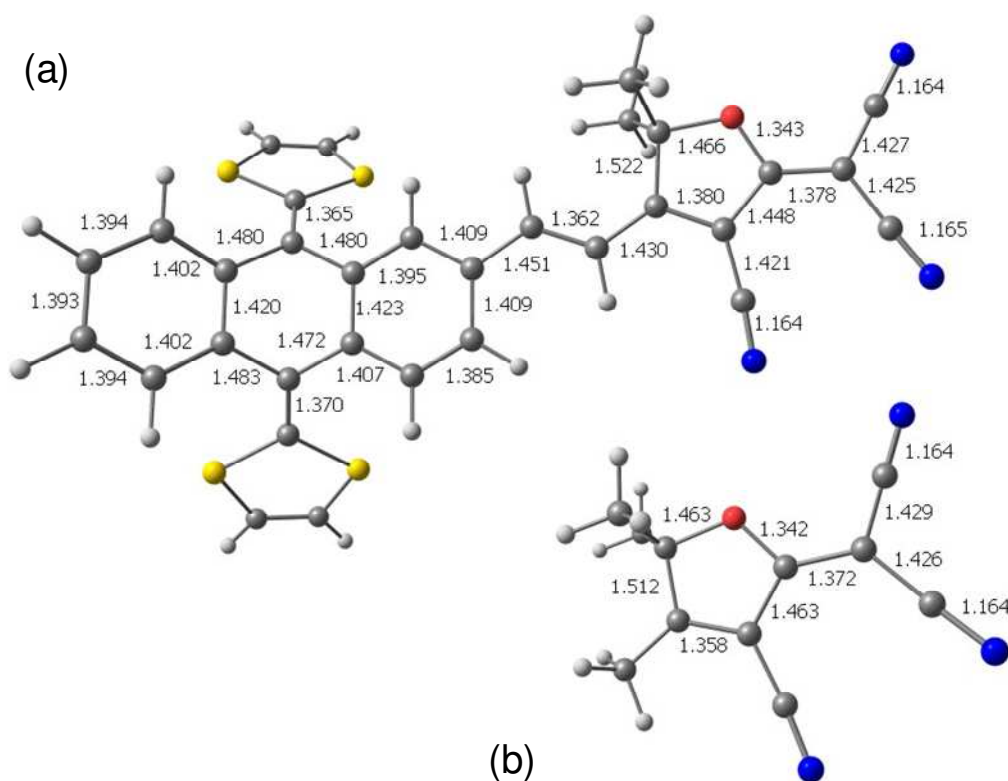

Figure S7. B3LYP/6-31G**-optimized values calculated for selected bond lengths (in Å) of compounds **3a** (a) and **2** (b).

Vertical electronic transition energies were computed at the B3LYP/6-31G** level using the TDDFT approach[8] and the optimized ground-state molecular geometries. The vertical excitation energies were also calculated using the hybrid PBE0 functional.[9] As summarized in Table S2, the B3LYP and PBE0 functionals provide an identical description of the lowest-energy excited states. The PBE0 functional however leads to slightly higher excitation energies that are in better accord with experimental values (see the main text). This effect is particularly important for the first two excited states S_1 and S_2, which imply a charge transfer from the exTTF unit to the TCF–C=C moiety. Although both the B3LYP and the PBE0 functionals underestimate the energy of the HOMO→LUMO (S_1) and HOMO−1→LUMO (S_2) CT states, the performance of these functionals for compounds **3** is quite good –the deviation from experiment is of only 0.3 eV (B3LYP) and 0.2 eV (PBE0)– because there exists a significant overlap between the HOMO/HOMO−1 of the donor and the LUMO of the acceptor (see Figure 2). The long-range corrected CAM-B3LYP functional,[10] that is usually recommended to deal with donor-acceptor systems, was also utilized to calculate the electronic absorption spectrum of **3a**. However, the CAM-B3LYP approach completely fails in reproducing the spectrum of **3a** since: i) the low-energy CT states are calculated too high in energy at 2.56 eV (400 nm) and 3.14 eV (395 nm), strongly underestimating the experimental excitation energies of 1.95 eV (635 nm) and 2.48 eV (499 nm), ii) the CT states are computed to be among the most intense ($f = 0.51$ and 0.72, respectively) electronic transitions in contradiction with experimental data, and iii) the absorption of the exTTF unit is calculated too high in energy at 340 nm largely below the experimental value around 400 nm.

TDDFT-PBE0/6-31G** calculations were also performed in the presence of the solvent to study the influence of solvent polarity on the electronic absorption spectrum. Solvent effects were considered within the SCRF (self-consistent reaction field) theory using the polarized continuum model (PCM)[11] approach to model the interaction with the solvent. The PCM model considers the solvent as a continuous medium with a dielectric

[8] a) Casida, M. E.; Jamorski, C.; Casida, K. C.; Salahub, D. R. *J. Chem. Phys.* **1998**, *108*, 4439–4449. b) Jamorski, C.; Casida, M. E.; Salahub, D. R. *J. Chem. Phys.* **1996**, *104*, 5134–5147. c) Petersilka, M.; Grossmann, U. J.; Gross, E. K. U. *Phys. Rev. Lett.* **1996**, *76*, 1212–1215.

[9] a) Ernzerhof, M.; Scuseria, G. E. *J. Chem. Phys.* **1999**, *110*, 5029–5036. b) Adamo, C.; Barone, V. *J. Chem. Phys.* **1999**, *110*, 6158–6170.

[10] Yanai, T.; Tew, D. P.; Handy, N. C. *Chem. Phys. Lett.* **2004**, *393*, 51–56.

[11] a) Tomasi, J.; Persico, M. *Chem. Rev.* **1994**, *94*, 2027–2094. b) Cramer, C. S.; Truhlar, D. G. *Solvent Effects and Chemical Reactivity*, Kluwer, Dordrecht, **1996,** pp 1–80.

constant ε, and represents the solute by means of a cavity built with a number of interlaced spheres.[12] The solvents considered were toluene ($\varepsilon = 2.38$), THF ($\varepsilon = 7.58$), DCM ($\varepsilon = 8.93$), CH_3CN ($\varepsilon = 36.64$), and DMSO ($\varepsilon = 46.70$). PBE0 calculations in the presence of the solvent led to a description of the electronic absorption spectra identical to that obtained for the isolated molecule and confirm the charge transfer nature of the S_1 and S_2 excited states. The main effect of the solvent is a slight destabilization of the HOMO and thereby a reduction of the HOMO-LUMO energy gap that passes from 2.20 eV for the isolated molecule to 2.06 (toluene), 2.00 (THF), 2.13 (DCM), 2.00 (CH_3CN), and 1.99 eV (DMSO). The electronic transition to S_1 due to the HOMO→LUMO monoexcitation is therefore calculated at very similar energies in all solvents (toluene: 1.58 eV, THF: 1.53 eV, DCM: 1.54 eV, CH_3CN: 1.54 eV, DMSO: 1.52 eV) and no clear solvatochromic effect is predicted in agreement with experimental observations.

Table S1. Lowest singlet excited states calculated at the TD-DFT level for **3a**. Vertical excitation energies (E), oscillator strengths (f), dominant monoexcitations with contributions (within parentheses) greater than 10%, and description of the excited states are given.

State	E (eV)	f	Monoexcitations	Description
			B3LYP/6-31G**	
S_1	1.62	0.14	H → L (89 %)	exTTF → TCF–C=C
S_2	2.18	0.28	H–1 → L (91 %)	exTTF → TCF–C=C
S_3	2.88	0.87	H–2 → L (77 %)	TCF–C=C → TCF–C=C
S_4	3.02	0.27	H–2 → L+1(83 %)	exTTF → exTTF
S_5	3.24	0.01	H → L+2 (72 %)	exTTF → exTTF
			H–1 → L+1 (19 %)	exTTF → exTTF
S_6	3.35	0.18	H–3 → L (86 %)	Antr+TCF–C=C → TCF–C=C
			PBE0/6-31G**	
S_1	1.75	0.17	H → L (90 %)	exTTF → TCF–C=C
S_2	2.33	0.32	H–1 → L (92 %)	exTTF → TCF–C=C
S_3	2.99	0.92	H–2 → L (77 %)	TCF–C=C → TCF–C=C
S_4	3.12	0.28	H–2 → L+1(80 %)	exTTF → exTTF
S_5	3.37	0.01	H → L+2 (73 %)	exTTF → exTTF
			H–1 → L+1 (16 %)	exTTF → exTTF
S_6	3.50	0.19	H–3 → L (86 %)	Antr+TCF–C=C → TCF–C=C

[12] a) Miertus, S.; Scrocco, E.; Tomasi, J.; *Chem. Phys.* **1981**, *55*, 117–119. b) Miertus, S.; Tomasi, J. *J. Chem. Phys.* **1982**, *65*, 239–245. c) Cossi, M.; Barone, V.; Cammi, R.; Tomasi, J. *Chem. Phys. Lett.* **1996**, *255*, 327–335. d) Cances, E.; Mennucci, B.; Tomasi, J. *J. Chem. Phys.*, **1997**, *107*, 3032–3041. e) Barone, V.; Cossi, M.; Tomasi, J. *J. Comput Chem.* **1998**, *19*, 404–417. f) Cossi, M.; Scalmani, G.; Rega, N.; Barone, V. *J. Chem. Phys.* **2002**, *117*, 43–54.
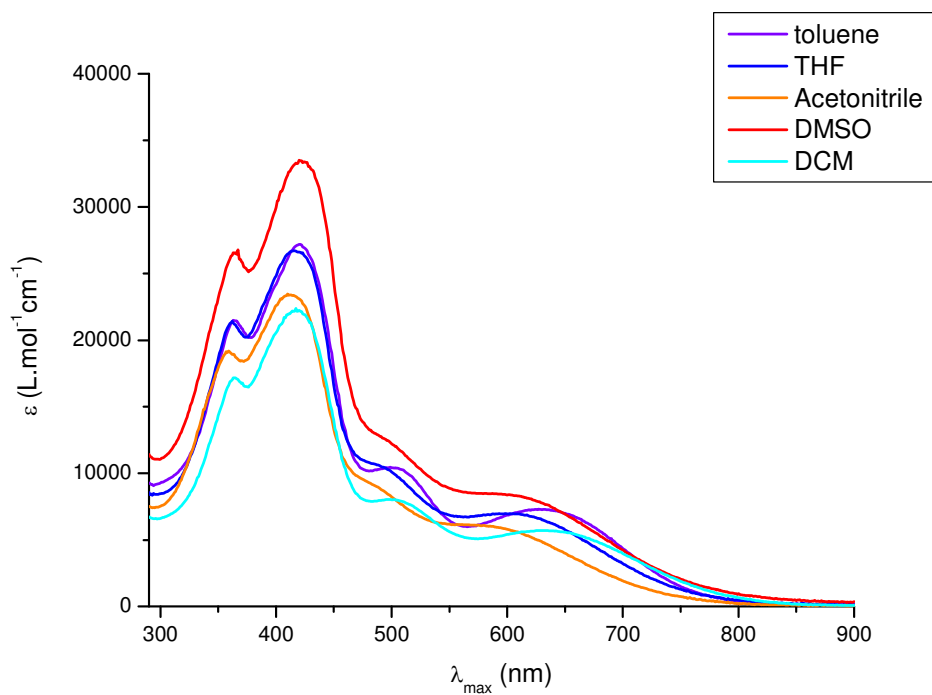
Solvatochromic study

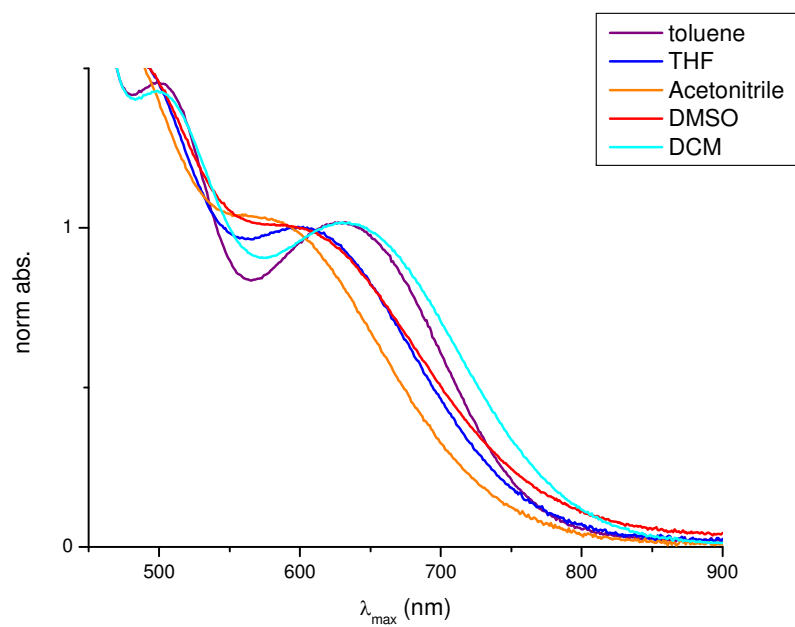**Figure S8.** Absorption spectra of **3a** recorded in different solvent at room temperature (c = 10^{-5}M.).

Figure S9. Normalized absorption spectra of **3a** recorded in different solvents at room temperature (c = 10^{-5}M.) in the 500-900 nm region.